# Implementation of Sic Based DC-DC Boost Converter for Photovoltaic Applications

A. Bharathi Sankar [1],
[1]Research scholar,
Department of Electrical & Electronics Engineering,
SSN college of Engineering Chennai,
Tamilnadu, INDIA.

Dr. R. Seyezhai [2]
[2] Associate Professor,
Department of Electrical & Electronics Engineering,
SSN college of Engineering Chennai,
Tamilnadu, INDIA.

***Abstract:-*** **Renewable energy source such as photovoltaic (PV) cell generate power from the sun light by converting solar power to electrical power with no moving parts, no maintenance. A single photovoltaic cell produces low level of voltage. In order to increase the magnitude of the voltage, dc-dc boost converter is used. In order to use this DC – DC converter for high voltage and high frequency applications, Silicon Carbide (SiC) device is the preferred choice. SiC power devices are preferred because of larger current carrying capability, higher voltage block capability, high operating temperature, and less static and dynamic losses than traditional silicon (Si) power switches. In the proposed work, PV & VI characteristics of the PV array with variation in temperature and irradiation levels. At various isolation and temperature levels, the load is varied and the corresponding variation in the voltage and current to the boost converter is noted. This DC - DC chopper is controlled using a Pulse-Width Method (PWM) and the duty cycle *d* is calculated for tracking the Maximum Power Point of the PV systems.Simulation studies are carried out in MATLAB/SIMULINK and the results are verified experimentally.**

## INTRODUCTION:

Power electronics are fundamental components in consumer electronics and clean energy technologies. For several decades, silicon (Si) has been the primary semiconductor choice for power electronic devices. Due to the many decades dedicated to the development and fabrication optimization of Si devices, as well as the large abundance of material, the manufacturing capability is high, and the costs are extremely low. However, Si is quickly approaching its limits in power conversion. Wide band gap (WBG) semiconductors offer promise of improved efficiency, reduced size, and lower overall system cost. Of the various types of WBG semiconductors, silicon carbide (SiC) have proven to be the most promising technologies, with several devices already being sold commercially [1].

Alternatively, SiC has shown tremendous high temperature capability, as well as aptitude for high voltage applications. Furthermore, the cost of SiC devices has decreased within the last decade, and the performance has proven superior to that of conventional Si devices. Some of the potential application areas for these WBG devices include: transportation electrification and renewable energy. Transportation electrification is a major trend today, especially in the automotive industries. Further success of electric vehicle automation on advances in power electronics. Regarding renewable energy, in particular, WBG devices have been explored for replacement of Si insulated gate bipolar transistors (IGBTs) in photovoltaic inverters in order to improve efficiency. WBG semiconductors are well suited for these applications due to their high temperature capabilities, fast switching speeds, and low losses. The high temperature capability of these devices allows them to better withstand the harsh environmental conditions, and have relaxed cooling system requirements. In addition to this high temperature capability, the fast switching speed of these devices allows for higher frequency operation thereby resulting in the reduction of the passive components, which decreases the total size, weight, and cost of the system [2].

These benefits of WBG semiconductors such as SiC arise from their greater thermal conductivity, higher critical electric field for breakdown and saturation electron drift velocity, and lower intrinsic carrier concentration compared to Si. The higher thermal conductivity of SiC makes it superior to Si in terms of heat transfer to the environment, which allows for increased power densities. SiC has a breakdown electric field that is more than eight times higher than that of Si. This means that, for a given blocking voltage, SiC can be more heavily doped than Si, thereby reducing the on-state resistance. The higher saturation drift velocity makes SiC more suitable for high frequency applications. Also, due to the wider band gap of SiC, it has a lower intrinsic carrier concentration, which allows these devices to operate at higher temperatures without suffering from excessive leakage.

Alternatively, the larger critical electric field for breakdown of SiC allows it to have a greatly reduced drift region resistance for the same breakdown voltage. Furthermore, SiC MOSFETs have the benefit of being unipolar devices, and thus typically experience faster switching than an IGBT. As a result, extensive work on the characterization of SiC MOSFETs, and comparison of their dynamic performance to Si IGBTs, has been carried out.

The SiC MOSFETs followed by detailed descriptions of the complete high temperature static and dynamic characterization methods and results [3].

The initial fabrication of SiC MOSFETs was stifled by two main issues: (1) the quality of the SiC/SiO2 interface, and (2) the high electric field generation. The poor quality of the boundary between the SiC surface and oxide resulted in low mobility in the inversion layer, while the high electric field generated within the SiC caused degradation of the gate oxide. Significant improvement has been made to the manufacturing of SiC MOSFETs, and thus it has been demonstrated that these issues have been resolved.

A common structure for SiC MOSFETs is the double-diffused or DMOSFET is shown in Figure 1, which allows for fast switching speed and high durability. In this structure, when no voltage is applied to the gate, a high voltage can be supported within the thick, lightly doped n-drift region. Upon application of a positive gate bias, an inversion layer is produced at the surface of the p- well region underneath the gate electrode. This inversion layer provides a path for the flow of current from the drain to the source. This structure includes an intrinsic body diode, and allows operation in both the first and third quadrants. Current flows through the body diode when the MOSFET gate is off, and a positive drain bias exceeding approximately 0.7 V is applied. If instead a positive gate voltage is applied, and the drain is negatively biased, then the channel will conduct with current flowing from the source to the drain, resulting in third quadrant operation [4].

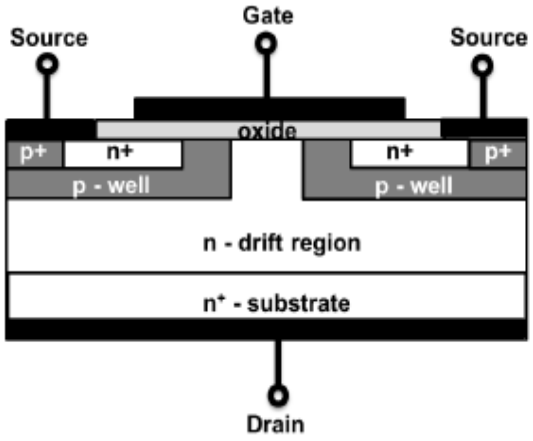


Figure 1 SiC MOSFET structure

The SiC power MOSFET is also capable of supporting high positive drain voltages. Furthermore, due to its greater critical electric field for breakdown, the doping concentrations in the drift region of SiC MOSFETs can be increased, thereby resulting in a lower drift resistance for a given blocking voltage. This relationship is shown by the following equation for the ideal on-state resistance Ron-ideal

$$R_{on-ideal} = \frac{4BV^2}{\varepsilon_s \mu_n E_C^3} \quad \ldots\ldots\ldots\ldots \quad (1)$$

Where BV is the breakdown voltage, $\varepsilon_s$ is the dielectric constant of the semiconductor, $\mu_n$ is the mobility of the drift region, and Ec is the critical electric field for breakdown. Moreover, SiC also features a higher saturation drift velocity, allowing for faster switching, and thus is suitable for high frequency applications.

## CHARACTERIZATION OF SIC MOSFET

Modeled SiC MOSFET static and dynamic characteristics are simulated using MATLAB. By extracting the parameters from the data sheet for various temperatures like 25C &150C.

### *Transfer Characteristics*

Transfer curve shows the variation of the drain current with respect to the gate source voltage as shown in figure 2.

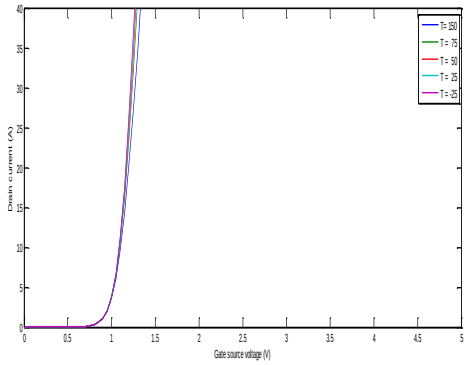


Figure 2: Transfer Characteristics of SiC MOSFET

### *Output Characteristics*

Output characteristic shows the variation of the drain current with respect to the drain source voltage as shown in figure 3 & 4.

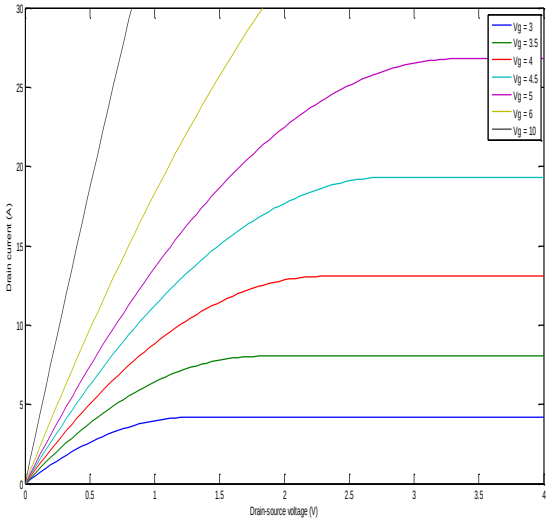


Figure 3: Output characteristics of SiC MOSFET at 25 C

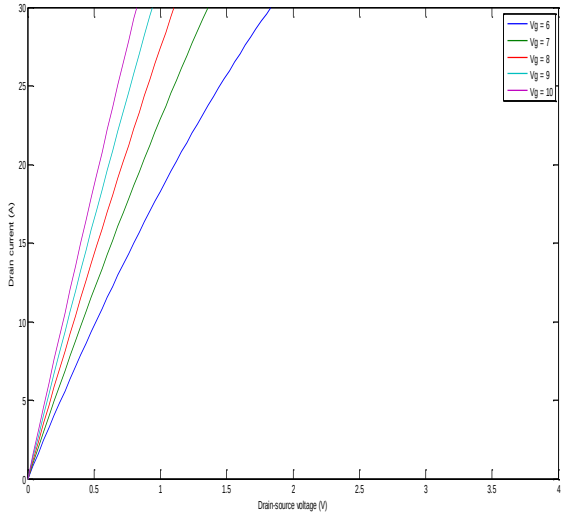


Figure 4: Output characteristics of SiC MOSFET at 150 C

## TEMPERATURE DEPENDENT BEHAVIOR COMPARISON BETWEEN SI AND SIC MOSFET

The $R_{DS}$ characteristic of Si and SiC MOSFET is shown in fig 5 and 6 respectively and the values for various temperatures between 0˚C to 150˚C.

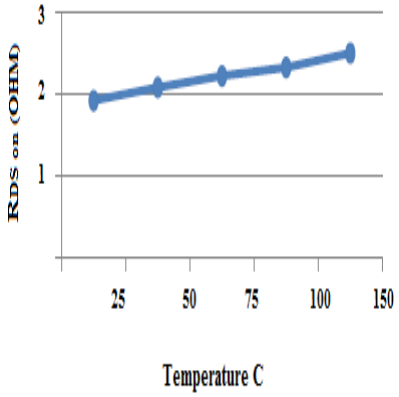


Figure 5: $R_{DS}$ characteristic of Si MOSFET

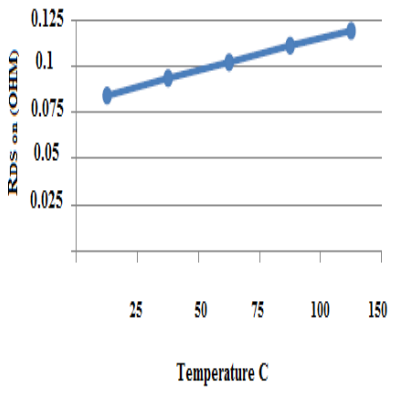


Figure 6: $R_{DS}$ characteristic of SiC MOSFET

## SWITCHING CHARACTERISTICS CURVE

Switching characteristics curve for SiC MOSFET is shown in fig 7 and it provides the information of the MOSFET under transient and saturation region and its corresponding dynamic parameters are shown in Table 1

Table 1: Dynamic parameters

| Parameter | Value |
|---|---|
| Turn on time ($t_{on}$) | 35 ns |
| Turn off time ($t_{off}$) | 76 ns |
| Fall time ($t_f$) | 36 ns |
| Rise time ($t_r$) | 22 ns |

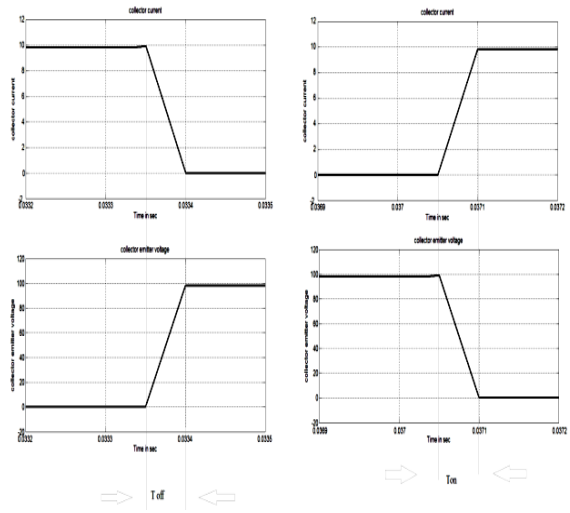


Figure .7 Determination of turn-on and turn-off time

## MAXIMUM POWER POINT TRACKING

The output efficiency of a photovoltaic cell is very low. In order to increase the output efficiency, different methods are to be analyzed to match the source and load side properly. So, to develop one such method is the Maximum Power Point Tracking control technique. This technique is used to obtain the maximum possible output power from a varying source power. In the photovoltaic systems, the V-I curve is non-linear, so it is difficult to get matched with the load. This technique is used for boost converter whose switching duty cycle is varied by using a Maximum power point tracking algorithm. A boost converter is used on the load side and a photovoltaic panel is used to power this converter. Various MPPT techniques are available in the literature, but this paper focuses on incremental conductance algorithm [5, 6].

## INCREMENTAL CONDUCTANCE METHOD

This method uses the photovoltaic panel incremental conductance dI/dV to compute the sign of dP/dV. When dI/dV is equal and opposite to the value of I/V (where dP/dV=0) the incremental conductance

algorithm knows that the maximum power point tracking control is reached and thus it terminates and returns the corresponding value of operating voltage for maximum power point. Flow chart of incremental conductance method is shown in Figure 8. This method tracks rapidly changing solar irradiation conditions more accurately than conventional method [7-10]. One complexity in this method is that it requires many sensors to operate and hence is economically less effective. Equations governing the proposed algorithm are as follows:

$$P = V * I$$

$$\frac{dP}{dV} = \frac{d(V*I)}{dV} \text{..... (2)}$$

$$\frac{dP}{dV} = I * \left(\frac{dV}{dV}\right) + V * \left(\frac{dI}{dV}\right) \text{ ..... (3)}$$

$$\frac{dP}{dV} = I + V * \left(\frac{dI}{dV}\right) \text{ ..... (4)}$$

When the MPPT is reached the slope

$$\frac{dP}{dV} = 0.$$

$$\frac{dP}{dV} = 0 \text{ ..... (5)}$$

$$I + V * \left(\frac{dI}{dV}\right) = 0 \text{ ..... (6)}$$

$$\frac{dI}{dV} = -\frac{I}{V} \text{ ..... (7)}$$

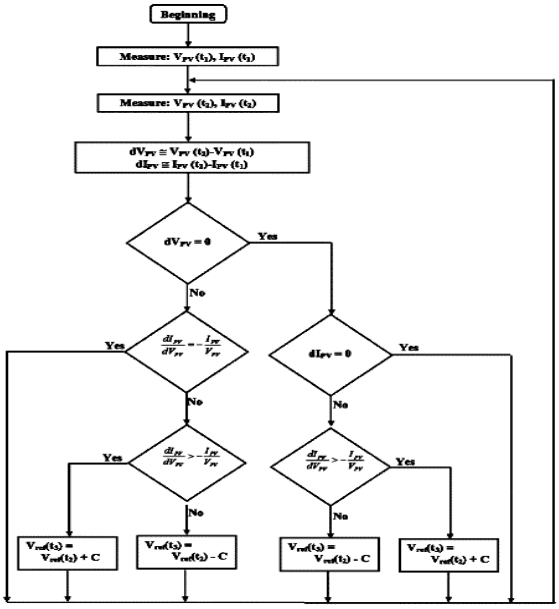


Figure 8: Flowchart of Incremental conductance method

## SiC MOSFET BASED BOOST DC-DC CONVERTER

Choppers are static DC-DC converters for generating variable DC voltage source from a fixed DC voltage source. It is used to step up the input voltage to a required output voltage without the use of a transformer. The control strategy lies in the manipulation of the duty cycle of the switch which causes the voltage change. The circuit diagram of the designed boost converter is shown in Figure.9.

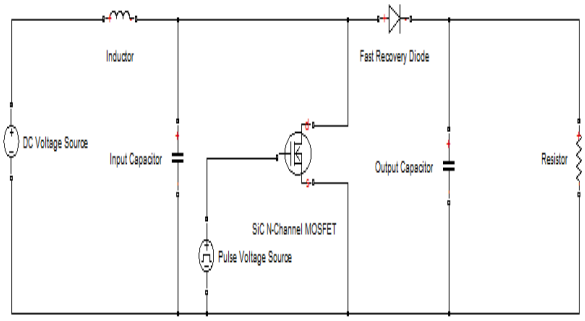


Figure 9: Circuit diagram of boost converter

The active switch in the boost converter is a 1200V SiC MOSFET. A fast recovery diode is used as the freewheeling diode. The input and output capacitor is selected as $C_1$ = 470µF and $C_2$ = 330 µF, 450 V .The inductance value is 2mH, 15 A. The functioning principle of the boost consist to excite the switch (SiC MOSFET) transistor with a duty cycle D produced by the IC based MPPT control, when the switch is closed the inductor L is loading during T(D) time, afterwards the switch is opened the inductor supplies the load R through the diode during (1-D)T. For a DC-DC boost converter, the input–output voltage relationship for continuous conduction mode is given by:

$$\frac{V_0}{V_{in}} = \frac{1}{1-D} \text{ ..... (8)}$$

Where, $D$ is the duty cycle since the duty ratio "$D$" is between 0 and 1. Simulink model of the IC based MPPT control of SiC DC– DC boost converter based photovoltaic power generation is shown in Figure.10.

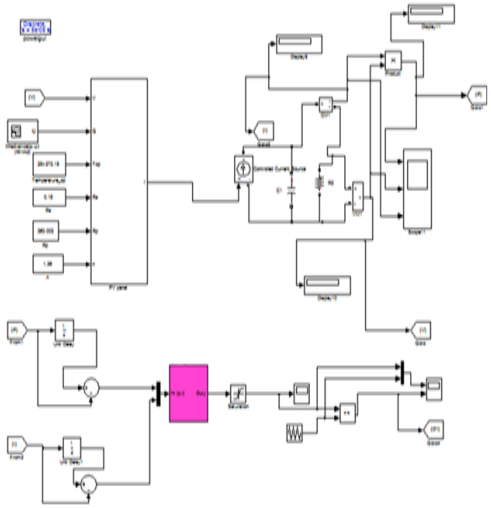

Figure 10: Simulink model of the IC MPPT control of SiC DC – DC boost converter based photovoltaic power generation

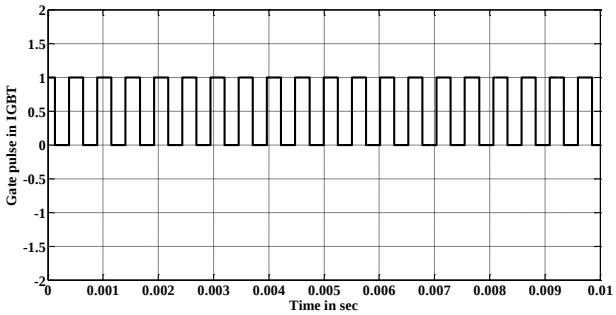


Figure .21: Gate pulse of SiC MOSFET

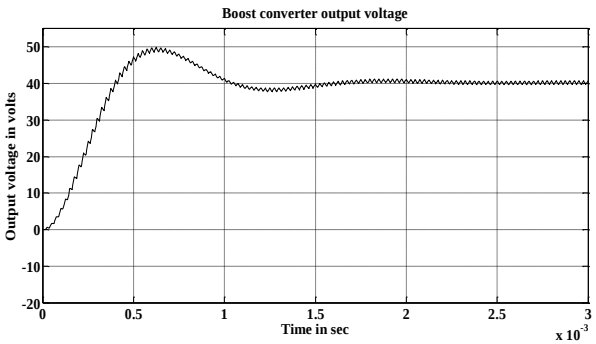


Figure .12: Output voltage of boost converter.

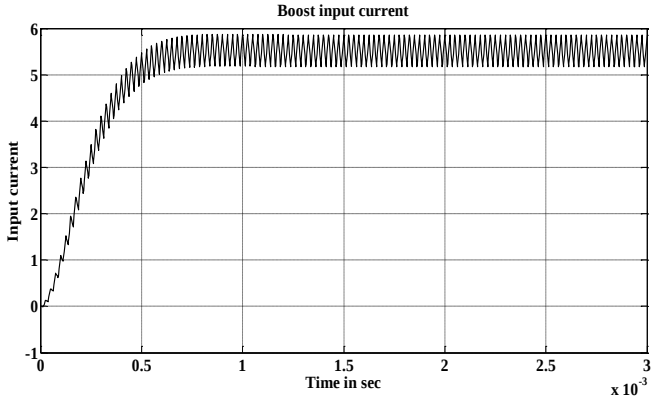


Figure .13: Input current of boost converter.

The DC- DC boost converter output voltage is about 44 Volts and input current of DC-DC boost converter is about 5 A as shown in Figures.12- 13.The gate pulse of SiC MOSFET switch with 50 % duty cycle is shown in Figure.11.

Table 2: Comparison between Si MOSFET and SiC MOSFET

| S.No | D % | SiC DC-DC Output voltage ripple % | Si DC-DC Output voltage ripple % | SiC DC-DC Input current ripple % | Si DC-DC Input current ripple % |
|---|---|---|---|---|---|
| 1 | 40 | 1.5 | 3.2 | 5.77 | 9.45 |
| 2 | 50 | 1.2 | 2.9 | 5.73 | 9.38 |
| 3 | 60 | 1.1 | 2.8 | 5.65 | 8.26 |
| 4 | 70 | 0.9 | 2.8 | 5.6 | 8.22 |

Table 2 shows the comparison between Si MOSFET and SiC MOSFET. By employing SiC MOSFET, it was found that the voltage ripple and input current are reduced compared to other techniques for the proposed system.

## EXPERIMENTAL SETUP OF PHOTOVOLTAIC POWER GENERATION

The hardware set-up for SiC MOSFET based photovoltaic power generation is shown in Figure.14.


Figure.15.Hardware set-up for IC based MPPT control based photovoltaic power generation system

In the experimental test conducted on photovoltaic panel with resistive load is shown in Figure.16. Photovoltaic panel specification is shown in table 3.It was observed photovoltaic panel output current and output voltage at various temperatures is shown in Table 4. The P-V and V-I characteristics for a photovoltaic panel are shown in Figure.17.

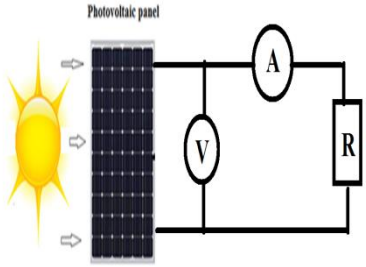


Figure 16.Experimental setup on photovoltaic panel

Table 3. Specification of PV Panel

| | |
|---|---|
| **$V_{oc}$** | 21.16 V |
| **$I_{sc}$** | 5.87 A |
| **$P_{max}$** | 95.32 W |
| **Insolation W/m$^2$** | 1000W/m$^2$ |
| **System efficiency** | 76.72 W |

Table 4.Voltage and current of PV at different time intervals

| Time | Voltmeter in volts | Ammeter in amps | Power in Watts |
|---|---|---|---|
| 10 am | 19.5 | 5.0 | 98 |
| 11 am | 20 | 5.1 | 102 |
| 12 pm | 20.3 | 5.2 | 103 |
| 1 pm | 20.2 | 5.2 | 103 |
| 2 pm | 20 | 5.1 | 102 |
| 3 pm | 19 | 5.0 | 95 |

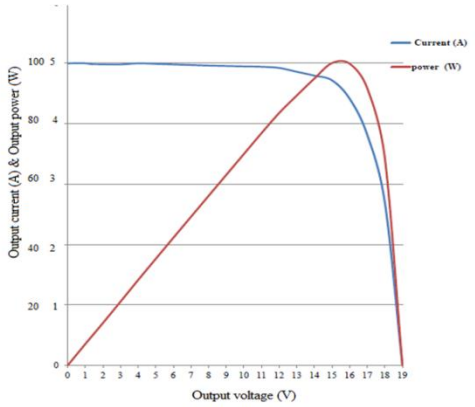


Figure 17: P-V & V-I characteristics of a photovoltaic panel

## IMPLEMENTING IC BASED MPPT ON FPGA

The IC based MPPT is implemented on the FPGA board. Then, the DC-to-DC is hooked up and connected to FPGA [11-14]. Figure.18 shows the logic circuit diagram in Xilinx ISE 14.1 software for the IC based MPPT and other components. The output of the controller is connected with a PWM module designed on the FPGA. The experimental PWM frequency of the modulating signal is about 50 KHz. The output of the PWM is examined using DSO by changing the values of the MPPT as shown in Figure. 19.

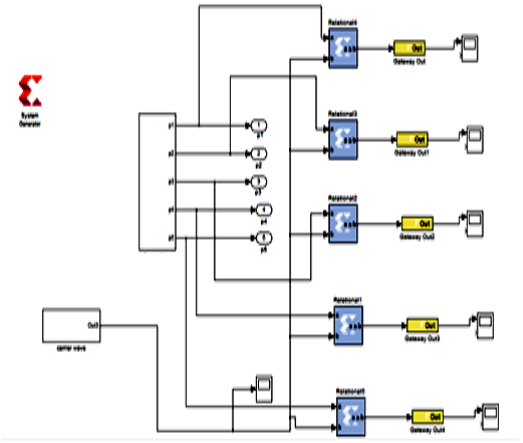

Figure 18: The logic circuit diagram in Xilinx software for the MPPT.

**50 % duty cycle**

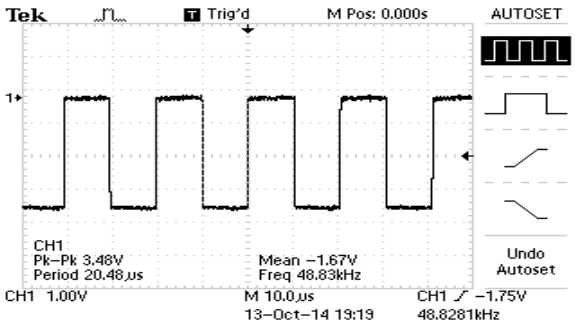


Figure.19. The change in the duty cycle of the PWM output

The hardware for the SiC MOSFET DC-DC converter is developed using SiC MOSFET –SCT 2080KE and fast recovery diode-MUR 3060.The input to the converter is about 19.5V and output voltage of DC-DC boost converter is about 40.9 V is shown in Figure.20.The SiC MOSFET switches at 50 % duty cycle. The output of the DC-to-DC converter is examined using the oscilloscope by the values of the MPPT inputs as an open loop and observe the change in the duty cycle of the PWM output and the change in the boost converter output as shown in Table 5.Output voltage ripple of SiC DC-DC boost converter is about 1.2 % is shown in Figure.21.


Figure 20.Input and Output voltage of step up boost converter using MPPT.

Table 5: The boost converter output in the various duty cycle of the PWM

| S.NO | $V_{IN}$ volt | $V_{OUT}$ volt | Duty Cycle % | Output voltage ripple % |
|---|---|---|---|---|
| 1 | 19.5 | 37.4 | 40 | 1.5 |
| 2 | 19.5 | 40.9 | 50 | 1.2 |
| 3 | 19.5 | 43.3 | 60 | 1.1 |
| 4 | 19.5 | 46.8 | 70 | 0.9 |

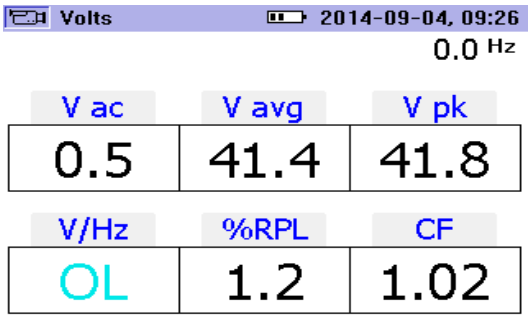


Figure 21. Output voltage ripple of SiC DC-DC boost converter for 50% duty cycle.

## CONCLUSION:

This paper has proposed a maximum power point tracker using incremental conductance MPPT implemented on FPGA Spartan-3E board for PV system. The proposed SiC MOSFET boost converter is tested using Matlab/Simulink and the results were compared with the conventional Si MOSFET and it is observed that the proposed converter gives a reduced output voltage ripple. Therefore the proposed SiC DC – DC boost converter is a suitable choice for photovoltaic power generation system.

## REFERENCES:

[1] *Jun, W., Z. Xiaohu. "10-kV SiC MOSFET-Based Boost Converter," IEEE Transactions on power electronics, 2008.*
[2] *McNutt, T., A. Hefner, et al. "Silicon Carbide Power MOSFET Model and Parameter Extraction Sequence," IEEE Transactions on power electronics, vol.22, no. 2, pp:217-226,MARCH 2007.*
[3] *Omura, M. Tsukuda, "High Power Density Converter using SiC-SBD," IEEE Transactions on power electronics , 2007.*
[4] *J. Wang, T. Zhao, J. Li, A. Q. Huang, R. Callanan, F. Husna, A. Agarwal, "Characterization, Modeling and Application of 10 kV SiC MOSFET," to be published in IEEE Trans. Electron Devices, Aug.2008.*
[5] *Mei Shan Ngan, Chee Wei Tan, "A Study of Maximum Power Point Tracking Algorithms for Stand-alone Photovoltaic Systems," IEEE applied power electronics colloquium, 2011.*
[6] *V. Salas, E. Oli´s, A. Barrado and A. La´zaro, "Review of the maximum power point tracking algorithms for stand-alone photovoltaic systems," Solar Energy Materials & Solar Cells (2006) 1555–1578.*
[7] *D. P. Hohm and M. E. Ropp, "Comparative Study of Maximum Power Point Tracking Algorithms," Programme of Photovoltaic Res. Application. 2003; Vol.11:47–62.*
[8] *Yinqing Zoua , Youling Yua, Yu Zhangb and Jicheng Luc, "MPPT Control for PV Generation System Based on an Improved Incremental conductance Algorithm," Procedia Engineering Vol.29 (2012) 105-109.*
[9] *Ahmad Al-Diab, Constantinos Sourkounis, "Variable Step Size P&O MPPT Algorithm for PV Systems," 2010, 12th International Conference on Optimization of Electrical and Electronic Equipment, OPTIM 2010.*
[10] *Eftichios Koutroulis, Kostas Kalaitzakis and Nicholas C. Voulgaris, "Development of a Microcontroller-Based, Photovoltaic Maximum Power Point Tracking Control System," IEEE transactions on power electronics, Vol. 16, No. 1, January 2001.*
[11] *Khaehintung N, Wiangtong T, Sirisuk P,"FPGA Implementation of MPPT Using Variable Step-Size P&O Algorithm for PV Applications", IEEE International Symposium on Communication and Information, IEEE-ISCIT 06,212-215. 2006.*
[12] *Mekki H., Mellit A., Kalogirou S.A., Messai A. and Furlan, G. FPGA-Based implementation of a real time photovoltaic module simulator, Progress in Photovoltaics: Research and Application, 2010, 18: 115-127.*
[13] *Messai, A. Mellit, A. Guessoum, and S.A. Kalogirou, "Maximum power point tracking using a GA optimized fuzzy logic controller and its FPGA implementation", Solar energy, 2010.*